

# Site Isolated Rh(II) Metalloradicals Catalyze Olefin Hydrosilylation

Zihang Qiu, Hao Deng, and Constanze N. Neumann\*

Max-Planck-Institut für Kohlenforschung, Kaiser-Wilhelm-Platz 1, 45470, Mülheim an der Ruhr, Germany.

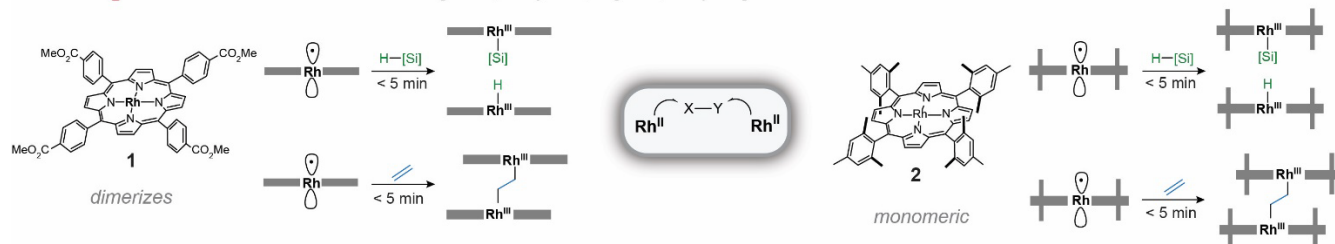
**KEYWORDS** Rh(II) metalloradicals, MOF site-isolation, hydrosilylation catalysis, MOF catalysis, catalyst deactivation prevention

**ABSTRACT:** Rh(II) porphyrin complexes display pronounced metal-centered radical character and the ability to activate small molecules under mild conditions, but catalysis with Rh(II) porphyrins is extremely rare. In addition to facile dimerization, Rh(II) porphyrins readily engage in kinetically and thermodynamically facile reactions involving two Rh(II) centers to generate stable Rh(III)-X intermediates that obstruct turnover in thermal catalysis. Here we report site isolation of Rh(II) metalloradicals in a MOF host, which not only protects Rh(II) metalloradicals against dimerization, but also allows them to participate in thermal catalysis. Access to PCN-224 or PCN-222 in which the porphyrin linkers are fully metalated by Rh(II) in the absence of any accompanying Rh(0) nanoparticles was achieved via the first direct MOF synthesis with a linker containing a transition-metal alkyl moiety, followed by Rh(III)-C bond photolysis.

Rh(II) porphyrins have attracted sustained interest due to reports of fascinating stoichiometric transformations, including activation of the C-H bond in methane at room temperature.<sup>1-3</sup> Cooperative reaction pathways involving two rhodium centers are considered a hallmark of Rh(II) metalloradical chemistry, and multiple tethered porphyrin ligands have been prepared via laborious routes to facilitate di-Rh transformations.<sup>4</sup> For many substrates, however, cooperative engagement by two Rh(II) centers gives rise to closed shell Rh(III) products that are stable up to ~ 200 °C and obstruct turnover in thermal catalysis (Fig. 1A).<sup>5-6</sup> Preventing a close approach between Rh centers would force substrates to engage with only a single Rh center and avert deactivation of Rh(II) catalysts. Isolation of Rh(II) centers also

prevents reversible dimerization, and thus increases the concentration of reactive, monomeric Rh(II). Rh(II) complexes involving sterically bulky porphyrins, such as **2**, are protected against dimerization via Rh-Rh bond formation, but reactions between two Rh centers and a substrate to yield closed-shell products remain facile.<sup>7</sup> Site-isolation of Rh(II) in a MOF, on the other hand, prevents all reactions involving two Rh centers, and thus substantially alters the mode in which Rh(II) engages with both silanes and olefins (Fig. 1B). We show that MOF heterogenization of Rh(II) porphyrins enables thermal hydrosilylation catalysis, renders light-promoted catalysis notably more efficient, and increases the selectivity with which the hydrosilylated product is formed.

## A Homogeneous Rh<sup>II</sup> Metalloradicals [Chan, Wayland, Ogoshi, Halpern]



## B Site-Isolated Rh<sup>II</sup> Metalloradicals [this work]

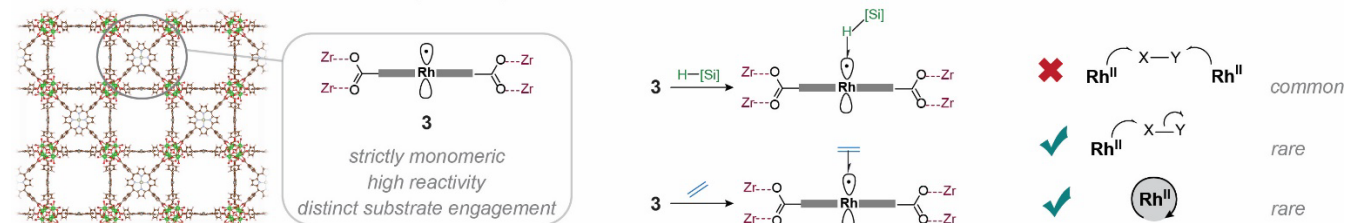


**Figure 1.** Unlike reported homogeneous systems,<sup>7-11</sup> MOF-based Rh(II) porphyrins catalyze olefin hydrosilylation.

Well-defined heterogenization of transition metal catalysts in MOFs or on high surface area supports via surface organometallic chemistry has proven to be an effective strategy for the prevention of deactivation via catalyst dimerization or

ligand exchange.<sup>12-23</sup> Heterogenized catalysts can also display increased reaction rates if comparable homogeneous catalysts require sterically bulkier ligand environments to remain stable,

or if heterogenization improves the cooperation between a catalyst and a co-catalyst.<sup>18, 20, 24-29</sup> However, examples where site isolation alters the mode of substrate engagement by the catalyst are considerably rarer.<sup>30-32</sup> Notably, Lin and coworkers demonstrated that MOF-based catalysts could ensure substrate interaction with one,<sup>33</sup> or favoring two metal centers in two electron reactions.<sup>34-35</sup> Here we show that MOF site isolation can alter the course of radical reactions and thus eliminate facile radical recombination steps that lead to catalyst deactivation. To the best of our knowledge, thermal hydrosilylation with Rh(Me)-3 constitutes the first example where site isolation of a transition metal complex in a MOF is not only beneficial, but crucial for catalytic turnover.

There are few examples of Rh(II) metalloradical catalysis, and no prior report on Rh(II) porphyrin catalyzed intermolecular olefin hydrofunctionalization. The persistent challenge in Rh(II) porphyrin catalysis lies in the need to regenerate Rh(II) from stable Rh(III)-X intermediates formed in the catalytic cycle, for which the input of substantial amounts of energy by thermal (200 °C),<sup>5-6</sup> photochemical<sup>36-43</sup> or electrochemical<sup>44</sup> means is required. One notable exception to the high stability of Rh(III)-X intermediates obstructing catalytic turnover is Rh(III)-H, which can undergo facile cooperative reductive

elimination to furnish Rh(II).<sup>45-47</sup> Fang and coworkers demonstrated that Rh(II) porphyrin catalyzed synthesis of formamides from amines and CO was not only possible in the presence of a high-voltage mercury lamp, but also via thermal catalysis in the presence of 30 equivalents of Me<sub>2</sub>EtSiH as a sacrificial hydrogen atom donor.<sup>48</sup> Chan and co-workers also showed that Rh(III)-OH porphyrins can undergo cooperative reductive elimination of H<sub>2</sub>O<sub>2</sub> at 80 °C to regenerate Rh(II).<sup>49</sup> Reductive elimination from Rh(III)-OH enabled catalytic turnover of Rh(II) porphyrins in the C-C bond hydrogenolysis in [2.2]paracyclophane, but a reaction temperature of 200 °C was required to promote the challenging conversion of Rh(III)-C to Rh(III)-OH.<sup>6</sup>

Here we demonstrate that site-isolation prevents the formation of inert Rh(III)-C bonds so that a facile thermal pathway for Rh(II) catalyst regeneration becomes accessible that does not rely on the expulsion of H<sub>2</sub>. Consequently, hydrofunctionalization reactions such as hydrosilylation can be catalyzed without the need for excess silane. Furthermore, sterically unencumbered olefins, which are particularly prone to convert Rh(II) to inert Rh(III)-C intermediates (Fig. 1), are modified for the first time via Rh(II) porphyrin catalysis.

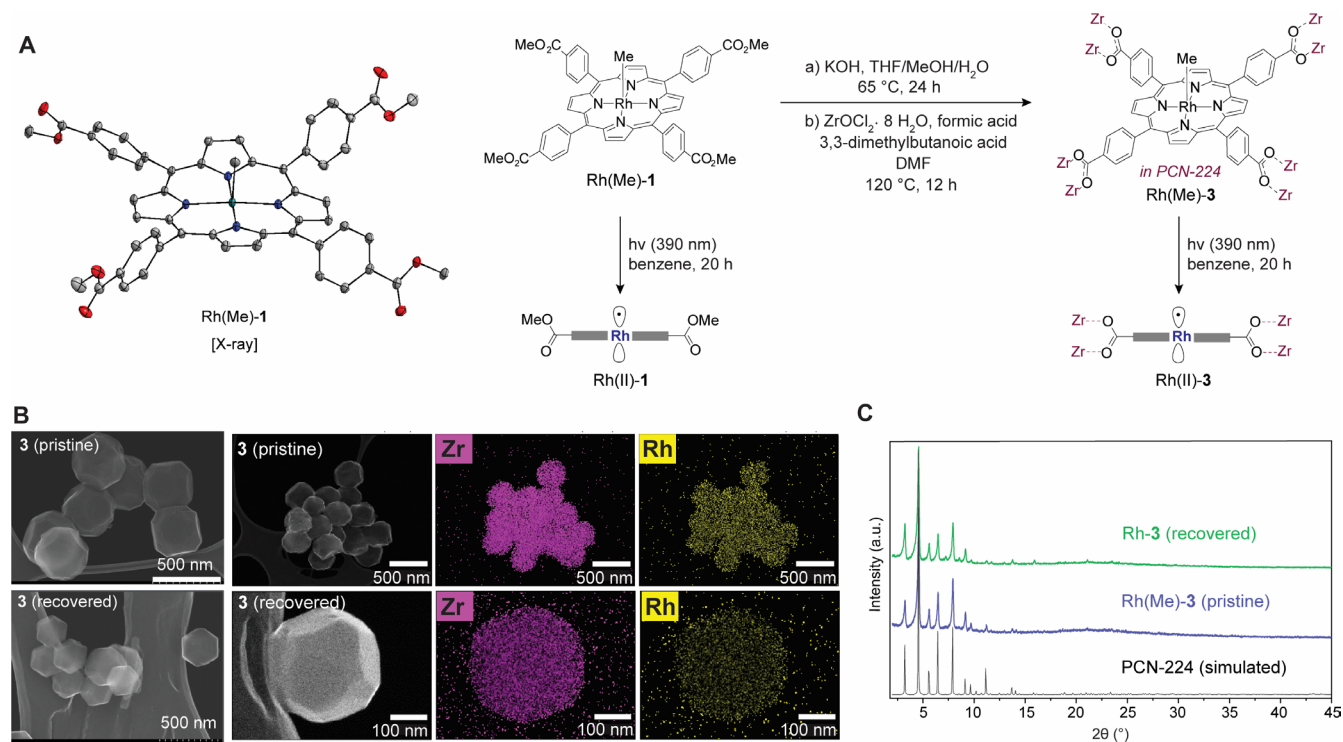


**Figure 2.** A Preparation of Rh(Me)-3 from Rh(Me)-1. B SEM images and EDX maps of pristine and recovered 3. C Comparison of PXR patterns for pristine and recovered 3. For details, please see Figures S13, S18–S23 and S119–120.

Given that MOFs are commonly prepared by hydrothermal synthesis, the installation of a reactive Rh(II) metalloradical center is challenging. We reasoned that Rh(II) may be accessed from the corresponding bench-stable Rh(III)-Me precursor via Rh-C photolysis.<sup>3</sup> When performed in benzene, Rh-C photolysis only generates methane and toluene alongside Rh(II), so that no side products are formed which are challenging to remove from the MOF host (Fig. S90–S92).<sup>21</sup> Metalation of porphyrin-linkers in MOFs has been reported with Rh(I),<sup>50</sup> and during the preparation of this manuscript, also with RhCl<sub>3</sub>.<sup>51</sup> Our initial attempts at the installation of Rh(III)-Me in pre-

formed PCN-222 or PCN-224 yielded porphyrin metalation alongside the formation of MOF-encapsulated nanoparticles that were invisible in PXR, and could not be removed by multiple washing cycles (Fig. S66–S87). The presence of low concentrations (<5% of total Rh content) of small Rh(0) nanoparticles is difficult to rule out experimentally,<sup>52</sup> and precursors known for porphyrin metalation (RhCl<sub>3</sub> or Rh<sub>2</sub>Cl<sub>2</sub>(CO)<sub>4</sub>) are also commonly used in Rh nanoparticle synthesis.<sup>4, 53-55</sup> Because Rh(0) nanoparticles and single rhodium atoms on oxide supports are able to activate silanes and catalyze hydrosilylation via

distinct reaction mechanisms than Rh(II) porphyrin centers, we aimed to avoid a post-synthetic metalation approach.<sup>56-58</sup>

Encouraged by the lack of Rh leaching during the synthesis of Rh(III)-Cl containing porphyrin MOFs reported by Zhang and Su,<sup>31, 59</sup> we developed a synthetic route involving MOF assembly from Rh(III)-Me containing porphyrin linkers (Fig. 2A, S12). Direct synthesis of organometallic MOFs is rare, with notable examples furnished by the groups of Yaghi and Wade.<sup>21, 60</sup> To the best of our knowledge, Rh(Me)-3 is the first example of MOF synthesis with a linker that contains a transition metal-alkyl moiety. To test the generality of direct MOF synthesis

with ligands that carry metal-alkyl bonds, we furthermore prepared Rh(Me)-4 (Fig. S40), for which the Rh center is site-isolated in the MOF host PCN-222. To characterize the ligand installed in the apical position on the rhodium center in Rh(Me)-3 and Rh(Me)-4 we obtained an X-ray structure of Rh(Me)-1 (Fig. 2, S148) used in the MOF synthesis, and characterized the MOFs by solid state NMR (Fig. S53–S60) as well as MOF digestion followed by LC-MS analysis (Fig. S26, S49) and NMR spectroscopy (Fig. S25, S48). Reproducible syntheses (Fig. S64–S65) of phase-pure Rh(Me)-3 and Rh(Me)-4 was ensured through the inclusion of a seed crystal of PCN-224 or PCN-222, respectively, a strategy developed by Zhou and co-workers.<sup>61</sup>

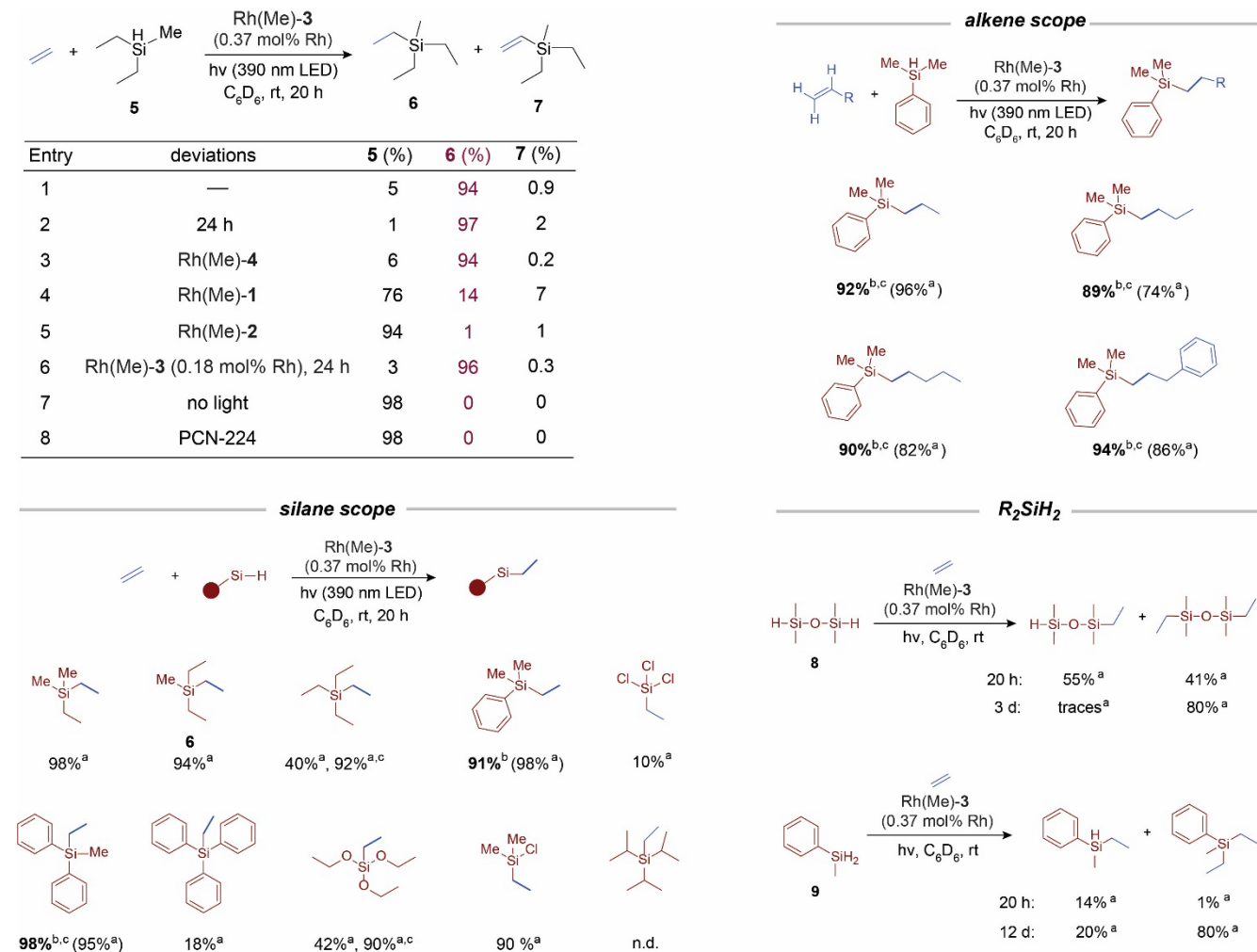


**Figure 3.** Evaluation of homogeneous (Rh(Me)-1, Rh(Me)-2) and MOF-based (Rh(Me)-3, Rh(Me)-4) catalysts and scope of olefin hydrosilylation catalyzed by Rh(Me)-3. Yields based on silane determined by (a) NMR or (b) isolation; reaction time increased to: (c) 2 d, (d) 3 d; see Supporting Information for experimental details (n.d.: not detected).

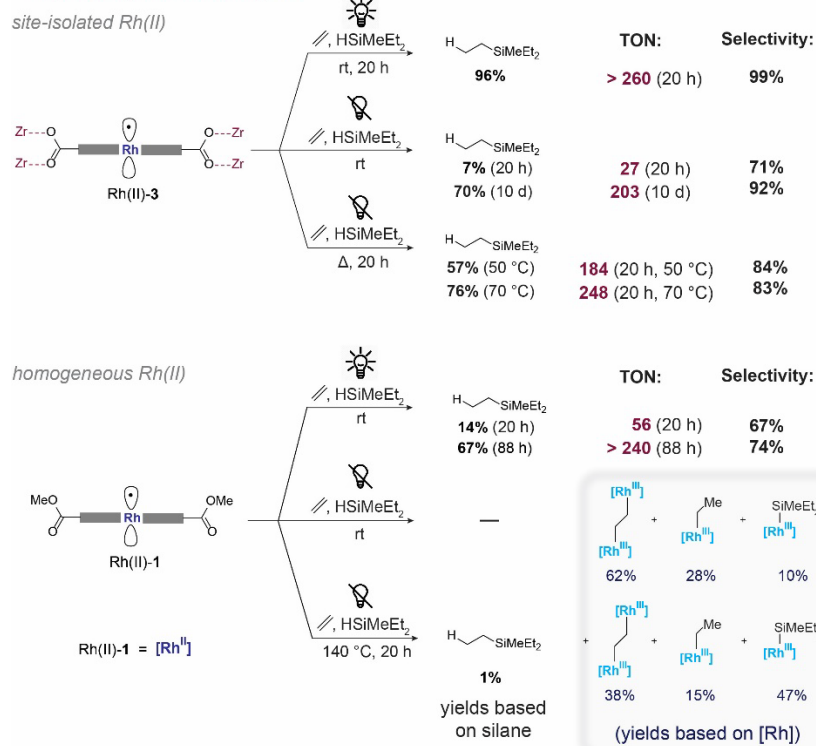
Simple illumination of Rh(Me)-3 with 390 nm LED light provided active catalyst Rh(II)-3, for which site-isolated Rh(II) metalloradicals are regularly spaced throughout the MOF framework. To compare the efficiency of MOF-based and homogeneous Rh(II) catalysts, we initially tested olefin hydrosilylation in the presence of light, since turnover for homogeneous Rh(II) catalysts commonly requires illumination.<sup>36-39</sup> Rh(Me)-1 serves as a homogeneous mimic of the Rh coordination environment present in the MOF-based catalysts Rh(Me)-3 and Rh(Me)-4. Additionally, we used Rh(Me)-2 to report on

the influence of Rh–Rh bond formation between metalloradicals (which is absent for Rh(II)-2, Rh(II)-3 and Rh(II)-4, but not Rh(II)-1) on catalytic performance. For Rh(Me)-3, a catalyst loading that corresponds to 0.37 mol% Rh was able to effect ethylene hydrosilylation in 94% yield, while homogeneous mimic Rh(Me)-1 furnished 6 in only 14% yield alongside 7% dehydrosilylated product 7 (Fig. 3). The presence of bulky substituents on the porphyrin ligand in Rh(Me)-2 further reduced catalytic efficiency (1% 6 formed), even though Rh(Me)-2 is monomeric in solution. An increase of the steric bulk of the ho-

homogeneous porphyrin catalyst thus failed to afford a more effective hydrosilylation catalyst, while MOF-supported Rh(Me)-**3** furnished 96% yield even when the catalyst loading was reduced to 0.18 mol% (Fig. 3, entry 6). Notably, MOF-based **3** could be reused at least 7 times with no systematic decrease in performance via simple centrifugation and decanting of the reaction mixture (Fig. S118). The combination of low catalyst loading and reusability is particularly important for rhodium-based catalysts given the scarcity and cost of the metal. Similarly to single-atom catalysts, MOF-based heterogeneous catalyst permit 100% usage of rhodium atoms, which is not possible with traditional supported heterogeneous catalysts.<sup>17</sup>

Since our focus was geared towards establishing the effect of site isolation of Rh(II) metalloradicals inside a MOF matrix on the facility of different catalytic steps in hydrosilylation, we

### A Hydrosilylation Catalysis



### B Formation of Rh–C or Rh–Si Bonds

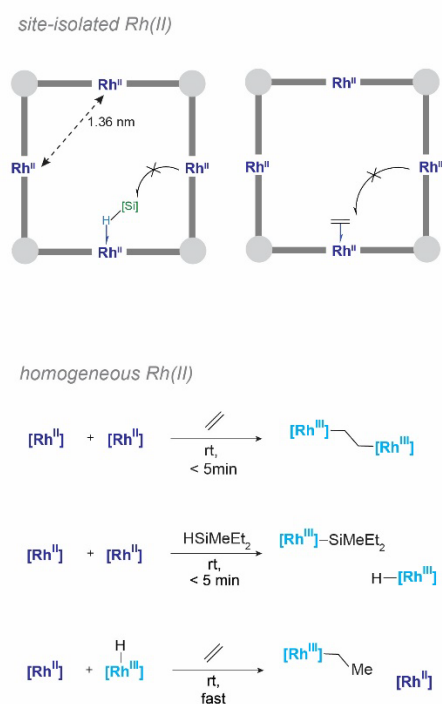


**Figure 4. Benefit of Rh(II) site isolation in catalytic hydrosilylation** **A** Catalytic hydrosilylation with MOF-based (Rh(II)-**3**) and homogeneous (Rh(II)-**1**) Rh(II) catalysts. **B** Undesirable side reactions that convert Rh(II) to thermally stable Rh(III) intermediates are prevented by site isolation (Fig. S129–S139).<sup>7-8, 11</sup>

Light is required for the formation of the active Rh(II) catalyst from the Rh(III)-Me precatalyst, but, once formed, Rh(II)-**3** is able to catalyze hydrosilylation of unactivated olefins at room temperature in the absence of light. Even though the reaction rate is slow, >200 turnovers could be achieved at room temperature. An increase of the reaction temperature permitted 184 turnovers (50 °C) or 248 turnovers (70 °C) after 20 h (Fig. 4A). For comparison, hydrosilylation reactions catalyzed by Mn(CO)<sub>5</sub> metalloradicals, which generate similar downstream intermediates, commonly require catalyst loadings of 5 mol% (TON ~ 20), as well as substantially higher reaction temperatures.<sup>62-63</sup> However, while homogeneous Mn(CO)<sub>5</sub> metalloradicals furnish effective hydrosilylation catalysis at elevated temperatures, Rh(II)-**1**, the homogeneous analogue of our MOF catalyst, furnished almost no hydrosilylated product. Three processes involving two Rh centers (Fig. 4B) are kinetically facile and sufficiently thermodynamically favorable that a reaction

primarily studied ethylene as the simplest, sterically unencumbered, and least electronically activated olefin substrate. However, the large pores of the PCN-224 MOF host of **3** also permit the use of bulkier olefin substrates (Fig. 3). Analogously to reported hydrosilylation reactions that proceed via silyl radical intermediates, internal alkenes such as 2-pentene (Fig. S115) proved unreactive. However, the apparent inability of the silyl radical to engage with non-terminal olefin positions ensured exclusive formation of the anti-Markovnikov product. Furthermore, bulky silanes and those bearing multiple chloride substituents provided <10% product, whereas HSi(OEt)<sub>3</sub> furnished high yields if the reaction time was extended to 3 d. Similarly, secondary silane (**9**) or oxygen-bridged disilane (**8**) required long reaction times, but furnished the corresponding bis-ethylene adducts in 80% yield.

temperature of 140 °C was unable to redirect the course of the reaction towards hydrosilylation. The use of light was more efficient at reversing side reactions involving two Rh centers, with 56 turnovers observed for Rh(II)-**1** after 20 h, and full silane conversion (TON > 240) after 88 h. For MOF-based Rh(II)-**3**, which does not generate inert off-cycle intermediates, full silane conversion (TON > 260) was reached after 20 h with 99% selectivity for the hydrosilylated product, versus 67–74% hydrosilylation selectivity for homogeneous analogue Rh(II)-**1**. The high productivity of MOF-based Rh(II)-**3** was particularly apparent at lower catalyst loadings, where 535 turnovers within 24 h furnished the hydrosilylated product in 96% yield (Fig. 3, entry 6).

We have shown that while reactions involving two Rh metalloradical centers are extremely facile (Fig. 4B), they furnish intermediates that are too unreactive to enable thermal hy-

drosilylation. The sterically bulky ligand environment of homogeneous catalyst **2** is able to prevent Rh–Rh dimerization, rendering **2** monomeric in solution, but it does not prevent two Rh centers engaging cooperatively with small molecules (Fig. S135–S139).<sup>7</sup> MOF-supported Rh centers behave as if they were present at infinite dilution in *all* reactions involving two Rh species, while an effective Rh concentration of  $\sim 0.5 \text{ mol}\cdot\text{L}^{-1}$  in the framework (Tab. S4) ensures that Rh – substrate reactions proceed efficiently. Despite the fact that Rh(II) porphyrins are well-known for their cooperative reaction pathways, we show here that in the case of olefin hydrofunctionalization, a strictly monomeric Rh(II) center is preferable for catalysis. The absence of side reactions involving two Rh centers in the MOF both expedites the light-promoted reaction, and enables thermal catalysis.

## ASSOCIATED CONTENT

The Supporting Information contains detailed experimental procedures, X-ray crystallographic data for Rh(Me)-**1** (CCDC-2286496), additional figures S1–S149, tables S1–S6, and NMR spectroscopic data.

## AUTHOR INFORMATION

Zihang Qiu ORCID: 0000-0002-8628-6497

Hao Deng ORCID: 0000-0002-8154-5314

Constanze N. Neumann ORCID: 0000-0003-1004-1140

## Corresponding Author

Email: \*neumann@kofo.mpg.de

## Author Contributions

The manuscript was written by Z.Q. and C.N.N. with contributions from all authors. All data was collected and analyzed by Z.Q. and H.D. with input from C.N.N. The project was conceived by Z.Q. and C.N.N. and directed by C.N.N.

## Funding Sources

Financial support was provided by the Lise-Meitner Program of the Max-Planck Society, an Alexander von Humboldt postdoc fellowship to Z.Q. and a China Scholarship Council (CSC) PhD scholarship to H.D.

## ACKNOWLEDGMENT

We thank the service departments of the Max-Planck-Institut für Kohlenforschung, in particular Dr. Markus Leutzsch and Dr. Christophe Farès (NMR), Heike Hinrichs (HPLC-MS), Jörg Rust and Dr. Nils Nöthling (scXRD), Daniel Margold, Dirk Kampen and Frank Kohler (mass spectrometry), and Hans-Josef Bongard and Alexander Kostis (electron microscopy). Helpful discussions with Prof. Tobias Ritter, and financial support from the Lise-Meitner program of the Max-Planck society, the Alexander von Humboldt foundation (postdoc fellowship to Z.Q.), and the CSC (PhD scholarship to H.D.) are gratefully acknowledged.

## ABBREVIATIONS

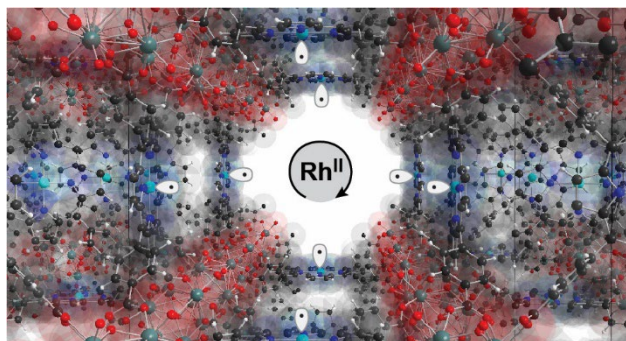
MOF, metal-organic framework; SEM, scanning electron microscopy; EDX, energy-dispersive X-ray spectroscopy; PXRD, powder X-ray diffraction; NMR, nuclear magnetic resonance, LC-MS, liquid chromatography-mass spectrometry; LED, light-emitting diode; TON, turnover number.

## REFERENCES

1. Cui, W.; Wayland, B. B., Activation of C–H/H–H Bonds by Rhodium(II) Porphyrin Bimetallo-radicals. *J. Am. Chem. Soc.* **2004**, *126* (26), 8266-8274.
2. Sherry, A. E.; Wayland, B. B., Metalloradical activation of methane. *J. Am. Chem. Soc.* **1990**, *112* (3), 1259-1261.
3. Cui, W.; Zhang, X. P.; Wayland, B. B., Bimetallo-Radical Carbon–Hydrogen Bond Activation of Methanol and Methane. *J. Am. Chem. Soc.* **2003**, *125* (17), 4994-4995.
4. Thompson, S. J.; Brennan, M. R.; Lee, S. Y.; Dong, G., Synthesis and applications of rhodium porphyrin complexes. *Chem. Soc. Rev.* **2018**, *47* (3), 929-981.
5. Chen, C.; Feng, S.; Chan, K. S., Rhodium Porphyrin Catalyzed Regioselective Transfer Hydrogenolysis of C–C  $\sigma$ -Bonds in Cyclopropanes with iPrOH. *Organometallics* **2019**, *38* (12), 2582-2589.
6. To, C. T.; Choi, K. S.; Chan, K. S., Catalytic Carbon–Carbon  $\sigma$ -Bond Hydrogenation with Water Catalyzed by Rhodium Porphyrins. *J. Am. Chem. Soc.* **2012**, *134* (28), 11388-11391.
7. Bunn, A. G.; Wayland, B. B., One-electron activation and coupling of ethene by rhodium(II) porphyrins: observation of an  $\mu^2$ -ethene-metalloradical complex. *J. Am. Chem. Soc.* **1992**, *114* (17), 6917-6919.
8. Feng, M.; Chan, K. S., Synthesis and reactivity of the non-bridged metal–metal bonded rhodium octamethoxyporphyrin dimer. *J. Organomet. Chem.* **1999**, *584* (2), 235-239.
9. Zhang, L.; Chan, K. S., Facile Synthesis of Rhodium(III) Porphyrin Silyls by Silicon–Hydrogen Bond Activation with Rhodium(III) Porphyrin Halides and Methyls. *Organometallics* **2006**, *25* (20), 4822-4829.
10. Mizutani, T.; Uesaka, T.; Ogoshi, H., Reactions of Rhodium Porphyrins with Lactones, Silanes, and Stannanes. *Organometallics* **1995**, *14* (1), 341-346.
11. Paonessa, R. S.; Thomas, N. C.; Halpern, J., Insertion and oxidative addition reactions of rhodium porphyrin complexes. Novel free radical chain mechanisms. *J. Am. Chem. Soc.* **1985**, *107* (14), 4333-4335.
12. Chabanas, M.; Baudouin, A.; Copéret, C.; Basset, J.-M., A Highly Active Well-Defined Rhenium Heterogeneous Catalyst for Olefin Metathesis Prepared via Surface Organometallic Chemistry. *J. Am. Chem. Soc.* **2001**, *123* (9), 2062-2063.
13. Chabanas, M.; Copéret, C.; Basset, J.-M., Re-Based Heterogeneous Catalysts for Olefin Metathesis Prepared by Surface Organometallic Chemistry: Reactivity and Selectivity. *Chem. Eur. J.* **2003**, *9* (4), 971-975.
14. Conley, M. P.; Mougél, V.; Peryshkov, D. V.; Forrest, W. P., Jr.; Gajan, D.; Lesage, A.; Emsley, L.; Copéret, C.; Schrock, R. R., A Well-Defined Silica-Supported Tungsten Oxo Alkylidene Is a Highly Active Alkene Metathesis Catalyst. *J. Am. Chem. Soc.* **2013**, *135* (51), 19068-19070.
15. Copéret, C.; Comas-Vives, A.; Conley, M. P.; Estes, D. P.; Fedorov, A.; Mougél, V.; Nagae, H.; Núñez-Zarur, F.; Zhizhko, P. A., Surface Organometallic and Coordination Chemistry toward Single-Site Heterogeneous Catalysts: Strategies, Methods, Structures, and Activities. *Chem. Rev.* **2016**, *116* (2), 323-421.
16. Musso, J. V.; De Jesus Silva, J.; Benedikter, M. J.; Groos, J.; Frey, W.; Copéret, C.; Buchmeiser, M. R., Cationic molybdenum oxo alkylidenes stabilized by N-heterocyclic carbenes: from molecular systems to efficient supported metathesis catalysts. *Chem. Sci.* **2022**, *13* (29), 8649-8656.
17. Iliescu, A.; Oppenheim, J. J.; Sun, C.; Dincă, M., Conceptual and Practical Aspects of Metal – Organic Frameworks for Solid–Gas Reactions. *Chem. Rev.* **2023**, *123* (9), 6197-6232.
18. Metzger, E. D.; Brozek, C. K.; Comito, R. J.; Dincă, M., Selective Dimerization of Ethylene to 1-Butene with a Porous Catalyst. *ACS Cent. Sci.* **2016**, *2* (3), 148-153.
19. Madrahimov, S. T.; Gallagher, J. R.; Zhang, G.; Meinhart, Z.; Garibay, S. J.; Delferro, M.; Miller, J. T.; Farha, O. K.; Hupp, J. T.;

- Nguyen, S. T., Gas-Phase Dimerization of Ethylene under Mild Conditions Catalyzed by MOF Materials Containing (bpy)Ni<sup>II</sup> Complexes. *ACS Catal.* **2015**, *5* (11), 6713-6718.
20. Zheng, H.; Fan, Y.; Song, Y.; Chen, J. S.; You, E.; Labalme, S.; Lin, W., Site Isolation in Metal–Organic Layers Enhances Photoredox Gold Catalysis. *J. Am. Chem. Soc.* **2022**, *144* (24), 10694-10699.
21. Burgess, S. A.; Kassie, A.; Baranowski, S. A.; Fritzsching, K. J.; Schmidt-Rohr, K.; Brown, C. M.; Wade, C. R., Improved Catalytic Activity and Stability of a Palladium Pincer Complex by Incorporation into a Metal–Organic Framework. *J. Am. Chem. Soc.* **2016**, *138* (6), 1780-1783.
22. Lee, J. S.; Kapustin, E. A.; Pei, X.; Llopis, S.; Yaghi, O. M.; Toste, F. D., Architectural Stabilization of a Gold(III) Catalyst in Metal–Organic Frameworks. *Chem* **2020**, *6* (1), 142-152.
23. Wang, Z.; Zeng, L.; He, C.; Duan, C., Metal–Organic Framework-Encapsulated Anthraquinone for Efficient Photocatalytic Hydrogen Atom Transfer. *ACS Appl. Mater. Interfaces* **2022**, *14* (6), 7980-7989.
24. Del Rosal, I.; Lassalle, S.; Dinoi, C.; Thieuleux, C.; Maron, L.; Camp, C., Mechanistic investigations via DFT support the cooperative heterobimetallic C–H and O–H bond activation across Ta–Ir multiple bonds. *Dalton Trans.* **2021**, *50* (2), 504-510.
25. Desai, S. P.; Ye, J.; Zheng, J.; Ferrandon, M. S.; Webber, T. E.; Platero-Prats, A. E.; Duan, J.; Garcia-Holley, P.; Camaioni, D. M.; Chapman, K. W.; Delferro, M.; Farha, O. K.; Fulton, J. L.; Gagliardi, L.; Lercher, J. A.; Penn, R. L.; Stein, A.; Lu, C. C., Well-Defined Rhodium–Gallium Catalytic Sites in a Metal–Organic Framework: Promoter-Controlled Selectivity in Alkyne Semihydrogenation to E-Alkenes. *J. Am. Chem. Soc.* **2018**, *140* (45), 15309-15318.
26. Zhang, X.; Llabrés i Xamena, F. X.; Corma, A., Gold(III) – metal organic framework bridges the gap between homogeneous and heterogeneous gold catalysts. *J. Catal.* **2009**, *265* (2), 155-160.
27. Fan, Y.; You, E.; Xu, Z.; Lin, W., A Substrate-Binding Metal–Organic Layer Selectively Catalyzes Photoredox Ene-Carbonyl Reductive Coupling Reactions. *J. Am. Chem. Soc.* **2021**, *143* (45), 18871-18876.
28. Zheng, H.; Fan, Y.; Blenko, A. L.; Lin, W., Sequential Modifications of Metal–Organic Layer Nodes for Highly Efficient Photocatalyzed Hydrogen Atom Transfer. *J. Am. Chem. Soc.* **2023**, *145* (18), 9994-10000.
29. Schlossarek, T.; Stepanenko, V.; Beuerle, F.; Würthner, F., Self-assembled Ru(bda) Coordination Oligomers as Efficient Catalysts for Visible Light-Driven Water Oxidation in Pure Water. *Angew. Chem. Int. Ed.* **2022**, *61* (52), e202211445.
30. Zhu, C.; Yuan, G.; Chen, X.; Yang, Z.; Cui, Y., Chiral Nanoporous Metal–Metallosalen Frameworks for Hydrolytic Kinetic Resolution of Epoxides. *J. Am. Chem. Soc.* **2012**, *134* (19), 8058-8061.
31. Epp, K.; Bueken, B.; Hofmann, B. J.; Cokoja, M.; Hemmer, K.; De Vos, D.; Fischer, R. A., Network topology and cavity confinement-controlled diastereoselectivity in cyclopropanation reactions catalyzed by porphyrin-based MOFs. *Catal. Sci. Technol.* **2019**, *9* (22), 6452-6459.
32. He, X.; Iliescu, A.; Yang, T.; Arguilla, M. Q.; Chen, T.; Kulik, H. J.; Dincă, M., Reversible O–O Bond Scission and O<sub>2</sub> Evolution at MOF-Supported Tetramanganese Clusters. *J. Am. Chem. Soc.* **2023**, *145* (30), 16872-16878.
33. Zhang, T.; Song, F.; Lin, W., Blocking bimolecular activation pathways leads to different regioselectivity in metal–organic framework catalysis. *Chem. Commun.* **2012**, *48* (70), 8766-8768.
34. An, B.; Li, Z.; Song, Y.; Zhang, J.; Zeng, L.; Wang, C.; Lin, W., Cooperative copper centres in a metal–organic framework for selective conversion of CO<sub>2</sub> to ethanol. *Nat. Catal.* **2019**, *2* (8), 709-717.
35. Lin, Z.; Zhang, Z.-M.; Chen, Y.-S.; Lin, W., Highly Efficient Cooperative Catalysis by Co(III)(Porphyrin) Pairs in Interpenetrating Metal–Organic Frameworks. *Angew. Chem. Int. Ed.* **2016**, *55* (44), 13739-13743.
36. Liu, X.; Liu, L.; Wang, Z.; Fu, X., Visible light promoted hydration of alkynes catalyzed by rhodium(III) porphyrins. *Chem. Commun.* **2015**, *51* (59), 11896-11898.
37. Liu, X.; Wang, Z.; Zhao, X.; Fu, X., Light induced catalytic hydrodefluorination of perfluoroarenes by porphyrin rhodium. *Inorg. Chem. Front.* **2016**, *3* (6), 861-865.
38. Yu, M.; Jing, H.; Liu, X.; Fu, X., Visible-Light-Promoted Generation of Hydrogen from the Hydrolysis of Silanes Catalyzed by Rhodium(III) Porphyrins. *Organometallics* **2015**, *34* (24), 5754-5758.
39. Yu, M.; Fu, X., Visible light promoted hydroxylation of a Si–C(sp<sup>3</sup>) bond catalyzed by rhodium porphyrins in water. *J. Am. Chem. Soc.* **2011**, *133* (40), 15926-9.
40. Wayland, B. B.; Poszmik, G.; Fryd, M., Metalloradical reactions of rhodium(II) porphyrins with acrylates: reduction, coupling, and photopromoted polymerization. *Organometallics* **1992**, *11* (11), 3534-3542.
41. Lee, S. Y.; Chan, K. S., Photocatalytic Carbon–Carbon  $\sigma$ -Bond Anaerobic Oxidation of Ketones with Water by Rhodium(III) Porphyrins. *Organometallics* **2013**, *32* (19), 5391-5401.
42. Liu, X.; Wang, Z.; Fu, X., Light induced catalytic intramolecular hydrofunctionalization of allylphenols mediated by porphyrin rhodium(III) complexes. *Dalton Trans.* **2016**, *45* (34), 13308-13310.
43. Bosch, H. W.; Wayland, B. B., The role of rhodium porphyrins in the photoassisted formation of formaldehyde and methanol from hydrogen and carbon monoxide. *J. Chem. Soc., Chem. Commun.* **1986**, (12), 900-901.
44. Natinsky, B. S.; Lu, S.; Copeland, E. D.; Quintana, J. C.; Liu, C., Solution Catalytic Cycle of Incompatible Steps for Ambient Air Oxidation of Methane to Methanol. *ACS Cent. Sci.* **2019**, *5* (9), 1584-1590.
45. Wayland, B. B.; Van Voorhees, S. L.; Wilker, C., Organometallic chemistry of rhodium tetraphenylporphyrin derivatives: formyl, hydroxymethyl, and alkyl complexes. *Inorg. Chem.* **1986**, *25* (22), 4039-4042.
46. Wayland, B. B.; Ba, S.; Sherry, A. E., Reactions of hydrogen or deuterium molecule with a rhodium(II) metalloradical: kinetic evidence for a four-centered transition state. *Inorg. Chem.* **1992**, *31* (1), 148-150.
47. Ogoshi, H.; Setsune, J.; Yoshida, Z., Hydridorhodium(III) porphyrin and porphyrin rhodium(II) dimer. *J. Am. Chem. Soc.* **1977**, *99* (11), 3869-3870.
48. Zhang, J.; Zhang, W.; Xu, M.; Zhang, Y.; Fu, X.; Fang, H., Production of Formamides from CO and Amines Induced by Porphyrin Rhodium(II) Metalloradical. *J. Am. Chem. Soc.* **2018**, *140* (21), 6656-6660.
49. Choi, K. S.; Lai, T. H.; Lee, S. Y.; Chan, K. S., Reduction of Rhodium(III) Porphyrin Hydroxide to Rhodium(II) Porphyrin. *Organometallics* **2011**, *30* (10), 2633-2635.
50. Szczepkowska, A. M.; Janeta, M.; Siczek, M.; Tylus, W.; Trzeciak, A. M.; Bury, W., Immobilization of Rh(i) precursor in a porphyrin metal–organic framework – turning on the catalytic activity. *Dalton Trans.* **2021**, *50* (26), 9051-9058.
51. Li, H.; Xiong, C.; Fei, M.; Ma, L.; Zhang, H.; Yan, X.; Tieu, P.; Yuan, Y.; Zhang, Y.; Nyakuchena, J.; Huang, J.; Pan, X.; Waagele, M. M.; Jiang, D.-e.; Wang, D., Selective Formation of Acetic Acid and Methanol by Direct Methane Oxidation Using Rhodium Single-Atom Catalysts. *J. Am. Chem. Soc.* **2023**, *145* (20), 11415-11419.
52. Finzel, J.; Sanroman Gutierrez, K. M.; Hoffman, A. S.; Resasco, J.; Christopher, P.; Bare, S. R., Limits of Detection for EXAFS Characterization of Heterogeneous Single-Atom Catalysts. *ACS Catal.* **2023**, *13* (9), 6462-6473.
53. Giordano, R.; Serp, P.; Kalck, P.; Kihn, Y.; Schreiber, J.; Marhic, C.; Duvail, J.-L., Preparation of Rhodium Catalysts Supported on Carbon Nanotubes by a Surface Mediated Organometallic Reaction. *Eur. J. Inorg. Chem.* **2003**, *2003* (4), 610-617.
54. Kim, T.-W.; Kim, M.-J.; Chae, H.-J.; Ha, K.-S.; Kim, C.-U., Ordered mesoporous carbon supported uniform rhodium nanoparticles as catalysts for higher alcohol synthesis from syngas. *Fuel* **2015**, *160*, 393-403.

55. Pan, H.-B.; Wai, C. M., Sonochemical One-Pot Synthesis of Carbon Nanotube-Supported Rhodium Nanoparticles for Room-Temperature Hydrogenation of Arenes. *J. Phys. Chem. C* **2009**, *113* (46), 19782-19788.
56. Sarma, B. B.; Kim, J.; Amsler, J.; Agostini, G.; Weidenthaler, C.; Pfänder, N.; Arenal, R.; Concepción, P.; Plessow, P.; Studt, F.; Prieto, G., One-Pot Cooperation of Single-Atom Rh and Ru Solid Catalysts for a Selective Tandem Olefin Isomerization-Hydrosilylation Process. *Angew. Chem. Int. Ed.* **2020**, *59* (14), 5806-5815.
57. Guo, W.; Pleixats, R.; Shafir, A.; Parella, T., Rhodium Nanoflowers Stabilized by a Nitrogen-Rich PEG-Tagged Substrate as Recyclable Catalyst for the Stereoselective Hydrosilylation of Internal Alkynes. *Adv. Synth. Catal.* **2015**, *357* (1), 89-99.
58. Solomonsz, W. A.; Rance, G. A.; Suetin, M.; La Torre, A.; Bichoutskaia, E.; Khlobystov, A. N., Controlling the Regioselectivity of the Hydrosilylation Reaction in Carbon Nanoreactors. *Chem. Eur. J.* **2012**, *18* (41), 13180-13187.
59. Liu, J.; Fan, Y.-Z.; Li, X.; Wei, Z.; Xu, Y.-W.; Zhang, L.; Su, C.-Y., A porous rhodium(III)-porphyrin metal-organic framework as an efficient and selective photocatalyst for CO<sub>2</sub> reduction. *Appl. Catal. B* **2018**, *231*, 173-181.
60. Oisaki, K.; Li, Q.; Furukawa, H.; Czaja, A. U.; Yaghi, O. M., A Metal–Organic Framework with Covalently Bound Organometallic Complexes. *J. Am. Chem. Soc.* **2010**, *132* (27), 9262-9264.
61. Xu, H.-Q.; Wang, K.; Ding, M.; Feng, D.; Jiang, H.-L.; Zhou, H.-C., Seed-Mediated Synthesis of Metal–Organic Frameworks. *J. Am. Chem. Soc.* **2016**, *138* (16), 5316-5320.
62. Dong, J.; Yuan, X.-A.; Yan, Z.; Mu, L.; Ma, J.; Zhu, C.; Xie, J., Manganese-catalysed divergent silylation of alkenes. *Nat. Chem.* **2021**, *13* (2), 182-190.
63. Yang, X.; Wang, C., Diverse Fates of  $\beta$ -Silyl Radical under Manganese Catalysis: Hydrosilylation and Dehydrogenative Silylation of Alkenes. *Chin. J. Chem.* **2018**, *36* (11), 1047-1051.
- 



Insert Table of Contents artwork here

---